

Slowly varying electromagnetic structures in a laser-plasma channel

A. Bigongiari, M. Borghesi, C. A. Cecchetti,
S. Kar and L. Romagnani

*School of Mathematics and Physics, Queen's University
Belfast, Belfast BT7 1NN, UK*

R. Jung, J. Osterholtz and O. Willi

Heinrich Heine University, Dusseldorf, Germany

T. V. Liseikina

*Max Planck Institute for Nuclear Physics,
Heidelberg, Germany*

A. Macchi

*polyLAB, CNR/INFM, Dept. of Physics 'E. Fermi',
Pisa, Italy*

M. Galimberti and R. Heathcote

*Central Laser Facility, STFC, Rutherford Appleton
Laboratory, HSIC, Didcot, Oxon OX11 0QX, UK*

Contact | m.borghesi@qub.ac.uk

Introduction

The generation of coherent and ordered structures is one of the most prominent phenomena in nonlinear many-body systems. Well-known examples are pattern formation, vortices or solitary waves, all these structures being relatively stable, i.e. evolving on time scales much longer than the typical times of the dynamics of the system. Theoretical studies have shown that plasmas, and particularly relativistic plasmas produced by the interaction with superintense laser pulses, provide several examples of electromagnetic (EM) coherent structures^[1]. These latter play an important part in the laser-plasma dynamics since a large fraction of the laser pulse energy can be converted into the slowly-varying, very intense electric and magnetic fields associated to such structures.

The development of the proton diagnostic technique^[2], providing direct information on EM fields in the plasma with high spatial and temporal resolution, has represented a turning point for the study of electromagnetic laser-plasma structures that previously could only be investigated numerically.

In this report, we present the analysis of proton imaging data of the interaction of a short (1.2 ps), high-intensity (up to $3 \cdot 10^{19}$ W/cm²) laser beam with a low density plasma, obtained using the Vulcan laser. As reported in a previous paper^[3], proton imaging data allowed a detailed study of the early stage of the interaction, which was characterised by the formation of a charge-displacement channel due to the ponderomotive action of the laser pulse and the subsequent evolution of the electrostatic, space-charge fields associated to the motion of the ions. Here we focus on later stages in the interaction, following the evolution over many picoseconds of the slowly varying electric and magnetic fields which are generated following the channel formation. In particular some features observed in experimental images can be explained by the presence of a solenoidal magnetic field around the channel which focuses probe protons along the axis on one side of the images. Regular patterns of bubble shaped structures, evolving over very long time scales compared to the typical dynamics of the plasma, are also observed. Their analysis is supported by two-dimensional (2D) particle-in-cell simulations showing patterns of long-lived electromagnetic structure, sharing

typical features of both magnetic vortices and electromagnetic 'cavitons' or 'post-solitons'^[4-6]. Particle tracing simulations show that 3D field configurations, built on the basis of the fields geometry resulting from 2D PIC simulations, produce proton projection images similar to the experimental ones.

Experimental setup

The experiment was carried out at the Rutherford Appleton Laboratory employing the Vulcan Nd-Glass laser system. The set-up has been already described in a previous paper^[3] where details can be found. Briefly, the interaction pulse (having 1.054 μ m wavelength and 1.3 ps duration) was focused by a *f*/6 parabola to achieve peak intensities up to $3 \cdot 10^{19}$ W/cm². The plasma was produced in a gas jet ionized by the 300 ps long prepulse, and interferometry was used to characterise the density profile. The latter was almost linearly rising along the axis of propagation of the laser pulse from a density of about 10^{18} cm⁻³ to a peak value of $1.3 \cdot 10^{19}$ cm⁻³ over a distance of 500 μ m.

The interaction pulse was synchronized with picosecond precision to a second pulse of similar intensity that was used to accelerate a proton beam for transverse probing of the interaction, under the Proton Projection Imaging scheme^[2]. Multilayered stacks of Radiochromic film (RCF) were used to detect the probe protons. On each film layer a 'proton image' is produced as a consequence of the deflections of the probe protons crossing the EM fields in the plasma. As the protons have a broad energy spectrum and each layer is sensitive to a different energy, in a time of flight arrangement a temporal series of 'proton images' is obtained for each single shot. The spatial and temporal resolution of each frame were of the order of a few picoseconds, and of a few microns, respectively, while the magnification was 11.

Proton images

Figure 1 shows proton images obtained respectively at times $t=17, 35$ and 140 ps ($t=0$ corresponds to the arrival of the pulse peak at the focal plane, $x=0$). Images obtained for earlier times show the propagation of the pulse front in the plasma and the formation of a charged channel along the axis, due to self-channeling^[3].

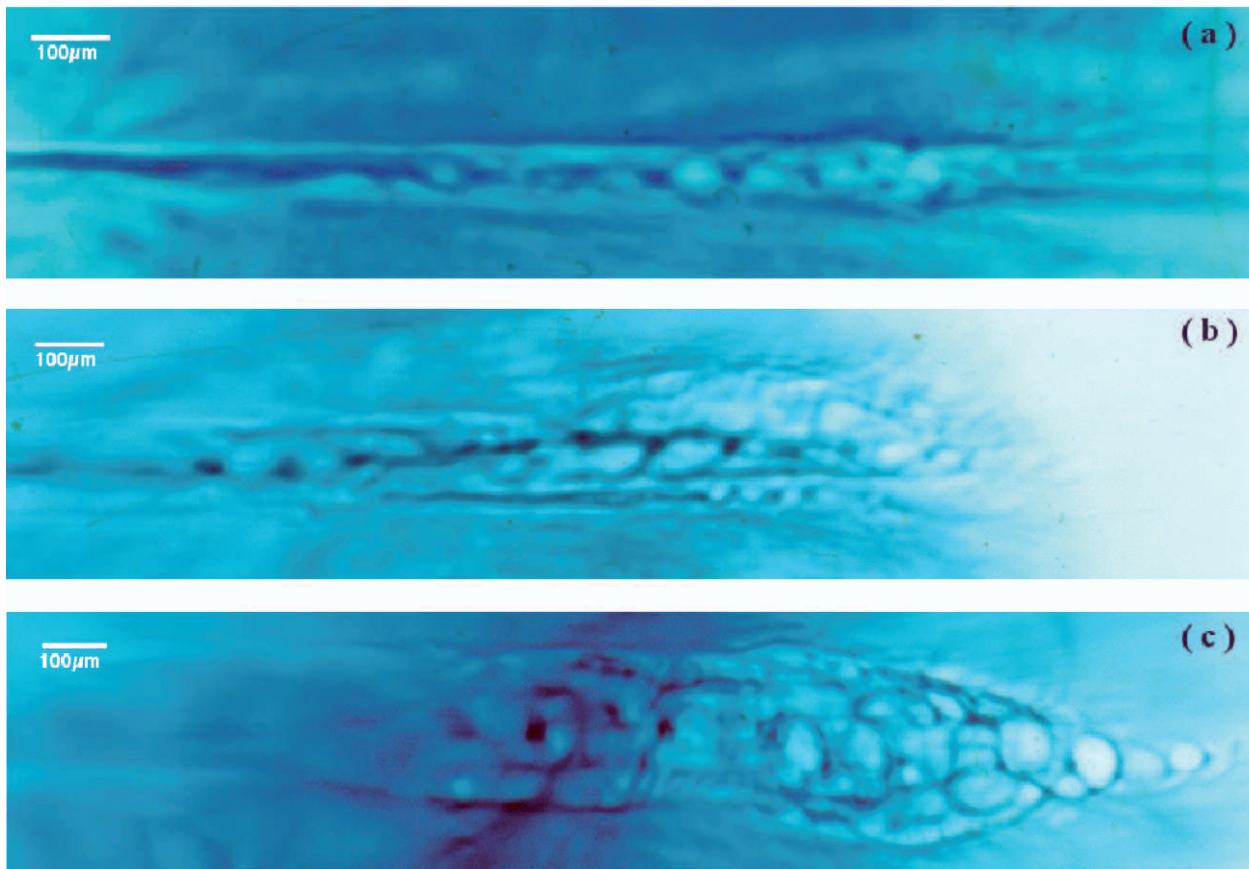


Figure 1. Proton images at various times after the laser pulse propagation: (a) 17 ps, (b) 35 ps (c) 140 ps, showing, at the earliest time, the ‘dark’ line along the channel axis on the left side of the image, and the evolution of ‘bubble’ structures, appearing inside the central channel first. The laser pulse propagates from left to right.

The image at $t=17$ ps shows that a few structures resembling ‘bubbles’ have formed inside the channel, in its central part. On the left side of such image a ‘black line’ appears along the axis. The later images ($t=35$ and 140 ps) suggest that both the channel and the ‘bubble’ structure inside expand, becoming fainter but remaining visible for long times (hundreds of ps).

PIC and particle tracing simulations

The experimental data can be qualitatively interpreted with the help of ‘particle-in-cell’ (PIC), two-dimensional (2D) simulations for a range of laser and plasma parameters close to those characterizing the experiments. The longest accessible simulation time was about 4.5 ps, significantly smaller than the time at which, for instance, ‘bubble’ structures are visible in proton images. Therefore, the PIC simulations give indications of the generation of field structures during the propagation of the laser pulse or soon after it, while the experimental observations are related to a later stage of the evolution of such structures.

In the PIC simulation results reported below, the electron density profile rises linearly from zero value at $x=25\lambda$ to the peak value $n_0=0.1n_c$ at $x=425\lambda$ and then remains uniform. The pulse duration is $300\lambda/c$, corresponding to 1 ps for $\lambda=1\mu\text{m}$. The laser pulse is S-polarized, i.e. the electric field of the laser pulse is in the z direction

perpendicular to the simulation plane and its peak field amplitude is $a=eE/m_c\omega c=2.7$. A wide discussion of simulation results in this regime is reported in ref.^[6].

The theoretical interpretation of the data was further supported by particle tracing simulations. The deflection of probe protons in given electromagnetic fields and the formation of proton images were simulated taking the experimental probe configuration into account. As the sensitivity of proton imaging technique is limited to quasi-static fields, only the latter were considered.

Magnetic fields in the plasma channel

We now discuss how the ‘black line’ observed in the left part of figure 1 at $t=17$ ps may be related to a solenoidal magnetic field around the laser channel. Figure 2 shows the magnetic field B_z , perpendicular to the simulation plane, at $t=1.5$ ps from the simulation start (i.e. when the laser pulse enters the simulation box from the left side). The electric current J_x in the propagation direction is also shown. The maximum amplitude of B_z is about 30 MGauss. The spatial profile of B_z in the wake of the laser pulse is consistent with the negative current along the axis, due to electrons accelerated inside the channel in the propagation direction, balanced by positive return currents flowing outside the channel. In a 3D geometry one thus expects an azimuthal magnetic field around the channel.

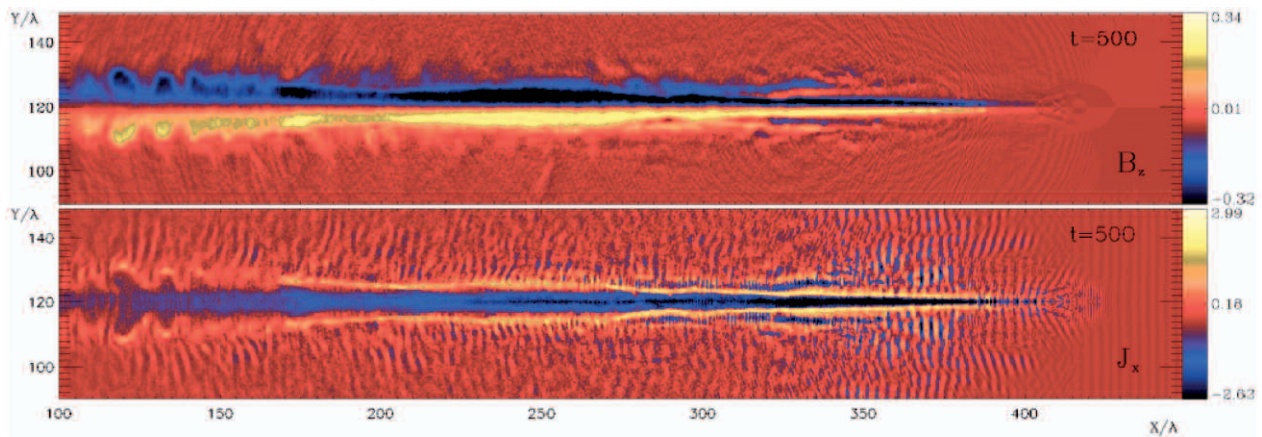


Figure 2. PIC simulation results showing the magnetic field B_z and the electric current J_x at $t=1.5$ ps.

Figure 3 shows a simulated proton projection corresponding to a field configuration resembling that found in the early stage of evolution of the plasma channel, i.e. consisting in a radial electric field of maximum intensity $3 \cdot 10^{11}$ V/m with a profile of the type discussed in ref. [3], and an azimuthal magnetic field of 10 MGauss around the axis. We obtain in this case a ‘white’ channel with a darker line along the axis, on the left part of the picture, indicating that the protons were focused toward the central region. According to particle tracing simulations using different electric and magnetic fields strength, this effect is mainly due to the magnetic field combined with the probe beam divergence. Probe protons having a speed component $v_x < 0$ (i.e. anti-parallel to the pulse propagation direction) tend to be focused towards the axis under the action of the azimuthal magnetic field, while protons having a parallel component ($v_x > 0$) are deflected in the opposite direction. Since the proton beam originates from a virtual point-like source, $v_x < 0$ holds for protons crossing the image plane at $x < 0$ while $v_x > 0$ for $x > 0$. Hence, probe protons will be focused near the axis and produce a ‘black line’ due to increased density on the RCF for $x < 0$, i.e. on the left side of the images shown in figure 1.

In ref. [3] it was shown that the radial electric field generated in the wake of the laser pulse has an ambipolar structure (originating from the effects of ion motion) and focus part of the probe protons on the axis (independently of their velocity) leading to a ‘black line’ as well. However, while it is plausible that in the initial stage electric field effects are predominant, the electric field decays quite rapidly in time and a major role at later times is played by the magnetic field that has a slower decay. This conclusion is supported by the persistence of the black line at quite long times and by its asymmetry in the images with respect to the $x=0$ plane.

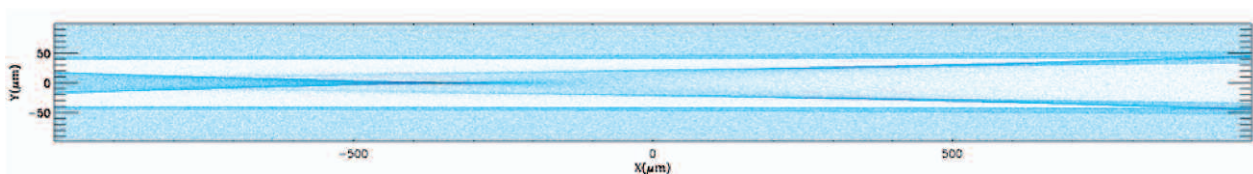


Figure 3. Simulated proton image from particle tracing in combined radial electric field and azimuthal magnetic field.

‘Bubble’ structures

We now focus on the ‘bubble’ structures that are visible inside the laser-plasma channel at $t=17$ ps in figure 1 and later expand. We trace these ‘bubbles’ back to patterns of slowly varying fields which in the 2D simulations are observed to grow inside the channel, and have been discussed in ref. [6]. The early stage of one of such patterns can be noticed on the left side of figure 2 and details of the field components B_z , E_x and E_y are shown in figure 4. The pattern of the slowly-varying magnetic field can be described as a double symmetrical row of magnetic vortices, ‘packed’ into the channel. The internal magnetic pressure causes the vortex to expand slowly sustaining a local depression of the density and a quasi-steady electrostatic field. Similar structures are observed also in the denser plasma region, inside narrow filaments that are originated from the main laser channel [6].

In principle, the electromagnetic structure defined by \mathbf{E}_0 and \mathbf{B}_0 is self-consistent, and the proton probe will be sensitive to such steady fields. Their origin might be due to instabilities associated to the repulsion of the counterpropagating electron currents; the differences in the vortex pattern with respect to previous numerical observations [6] might be ascribed to the different initial and boundary conditions, i.e. the presence of the channel and the separation between the current layers. It is however noticeable that the numerical simulations suggest a more complex or ‘hybrid’ structure, with the density depression associated to the vortex acting as a resonant cavity, i.e. trapping oscillating fields at a frequency just below the outside plasma frequency, as it is typical of ‘post-solitons’ [4]. The structure of the oscillating fields \mathbf{E}_ω and \mathbf{B}_ω is also shown in the cartoon of figure 4 and more details are given in ref. [6].

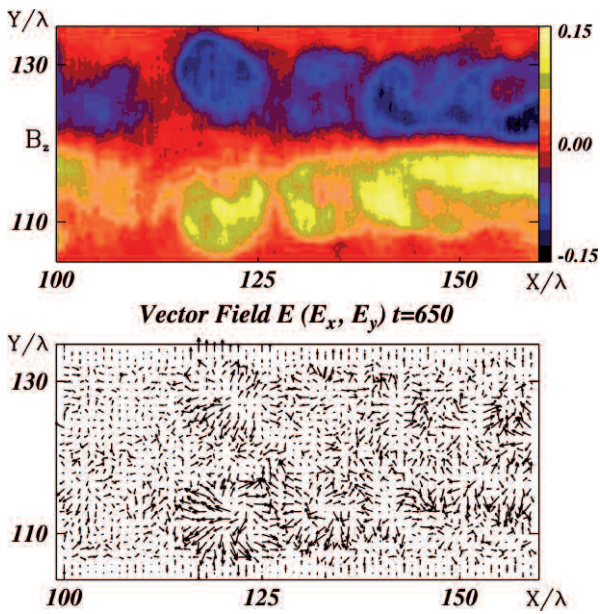


Figure 4. Detail from 2D PIC simulation.

On the basis of the 2D simulation results, we may imagine the real 3D topology of the steady fields associated to ‘bubble’ structures as having cylindrical symmetry and being qualitatively similar to what would have been obtaining by ‘rotating’ the schematic in figure 4 around the propagation axis. Such a 3D electric and magnetic field topology is shown in figure 5 and consists in a ‘doughnut’ shaped, axially symmetric magnetic field enclosed in a regular cavity generated as a modulation of the channel.

The resulting simulated PPIs using this field configuration are in good agreement with the experimental one (a detail is included in figure 5, showing white ‘bubble-shaped’ areas with darker contours).

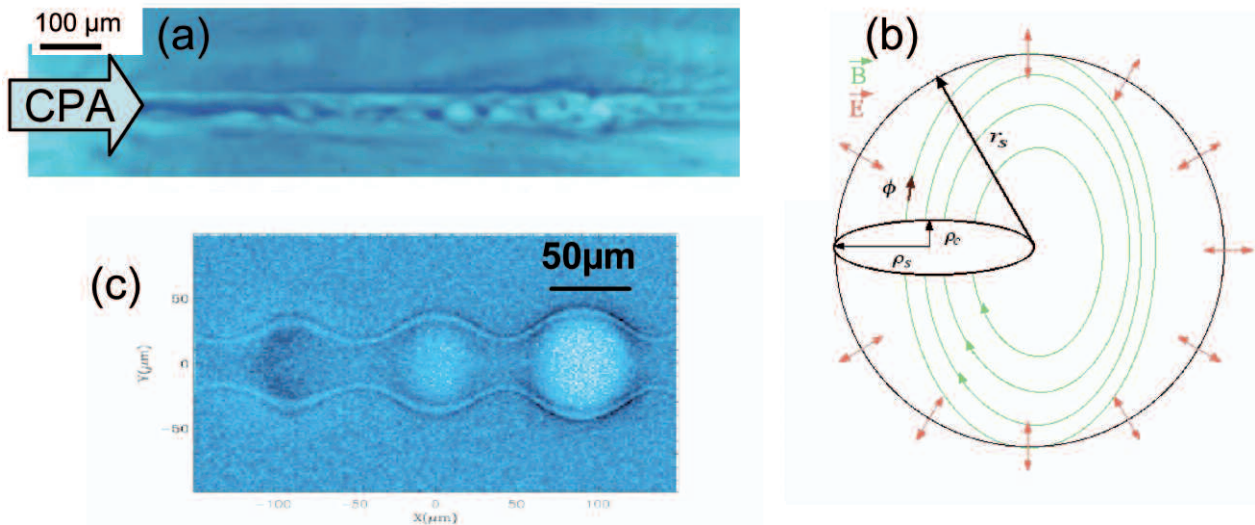


Figure 5. Simulated proton image from proton tracing simulations in an axially modulated electromagnetic field pattern (c) composed of a series of ‘doughnut’ structures as shown in (b). A detail of an experimental proton image (a) is included for comparison.

Conclusions

Slowly varying electromagnetic structures, surviving up to hundred of picoseconds, have been diagnosed by proton imaging around and inside a laser-plasma channel. Their analysis, performed with the help of PIC and particle tracing simulations, reveal a leading effect of self-generated magnetic fields and indicates the presence of patterns of coherent electromagnetic structures of a novel type.

References

1. S. V. Bulanov *et al.*, *Rev. Plasma Phys.* **22**, 227 (2001).
2. M. Borghesi *et al.*, *Rev. Sci. Instrum.* **74**, 1688 (2003).
3. S. Kar *et al.*, *New J. Phys.* **9**, 402 (2007).
4. M. Borghesi *et al.*, *Phys. Rev. Lett.* **88**, 135002 (2002).
5. S. V. Bulanov *et al.*, *Phys. Rev. Lett.* **76**, 3562 (1996).
6. A. Macchi *et al.*, *Plasma Phys. Control. Fusion* **49**, B71 (2007).